Journal of Low Temperature Physics (2020) 199:451–460
https://doi.org/10.1007/s10909-020-02398-2

Precision Measurements of Beta Spectra using Metallic Magnetic Calorimeters within the European Metrology Research Project MetroBeta

M. Loidl[1] · J. Beyer[2] · L. Bockhorn[3,5] · J. J. Bonaparte[4] · C. Enss[4] · S. Kempf[4] · K. Kossert[3] · R. Mariam[1] · O. Nähle[3] · M. Paulsen[2,4] · P. Ranitzsch[3] · M. Rodrigues[1] · M. Wegner[4]

Received: 19 July 2019 / Accepted: 8 February 2020 / Published online: 28 February 2020

Abstract

MetroBeta, a recently completed European Metrology Research Project, aimed at the improvement of the knowledge of the shapes of beta spectra, both in terms of theoretical calculation and measurement. The most prominent experimental work package concerned the measurement of the spectrum shapes of several beta decaying radionuclides by means of metallic magnetic calorimeters (MMCs) with the beta emitter embedded in the absorber. New MMC chips were designed and optimized for five different absorber heat capacities, enabling the measurement of beta spectra with Q values ranging from few tens of keV up to ~ 1 MeV. Several beta spectra were measured with high energy resolution and statistics of up to 10^7 counts.

Keywords Beta spectrometry · Metallic magnetic calorimeter · Radionuclide metrology

✉ M. Loidl
martin.loidl@cea.fr

[1] CEA, LIST, Laboratoire National Henri Becquerel (LNE-LNHB), CEA-Saclay, 91191 Gif Sur Yvette Cedex, France

[2] Physikalisch-Technische Bundesanstalt (PTB), Abbestrasse 2-12, 10587 Berlin, Germany

[3] Physikalisch-Technische Bundesanstalt (PTB), Bundesallee 100, 38116 Brunswick, Germany

[4] Kirchhoff-Institute for Physics, Heidelberg University, Im Neuenheimer Feld 227, 69120 Heidelberg, Germany

[5] Present Address: Institut für Festkörperphysik - Abteilung Nanostrukturen, Gottfried Wilhelm Leibniz Universität Hannover, 30167 Hannover, Germany

1 Introduction

There are several fields, including radionuclide metrology, nuclear medicine and the nuclear power industry, that request improved knowledge of beta spectrum shapes. In principle, there are two ways to determine the shapes of beta spectra: theoretical calculation or experimental beta spectrometry. Calculations of spectra from forbidden, in particular, non-unique transitions are very complicated, and spectra published in the literature often reveal large discrepancies for one and the same radionuclide. The theoretical approaches for improved calculations must be verified against precise experimental data.

Metallic magnetic calorimeters (MMCs) with beta emitters enclosed in noble metal absorbers have demonstrated their potential for the study of beta spectrum shapes [1–3]. In the European Metrology Research Project MetroBeta [4], MMCs were optimized for the requirements in beta spectrometry, and three beta spectra covering different types of beta transition have been measured: ^{14}C (allowed), ^{151}Sm (first forbidden non-unique) and ^{99}Tc (second forbidden non-unique). Measurements of ^{36}Cl (second forbidden non-unique) are under way.

2 Experimental

2.1 MMC Beta Spectrometry System

The development of MMCs within the project, optimized for absorber heat capacities ranging from 8 pJ/K to 1.7 nJ/K at 20 mK, has been described in Ref. [5]. Figure 1 shows the design of the "M size" (110 pJ/K) MMC chip together with a

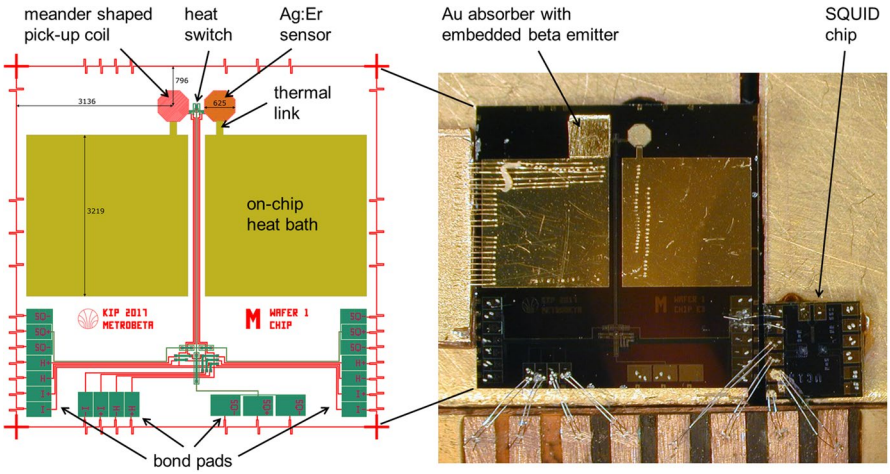

Fig. 1 *Left:* Design of the "M size" MMC chip. The chip size is (7.2 mm)^2. Some additional dimensions are given in the figure in µm; the sensor measures 625 µm across. For further details, see Ref. [6]. *Right:* Photograph of a chip from the first fabricated batch; a gold absorber with an embedded beta emitter is placed on one of the Ag:Er sensors. (Color figure online)

photograph of a chip from the first fabricated batch. A gold absorber with an embedded beta emitter is visible on one of the two Ag:Er sensors; it was fixed to the sensor with Stycast 1266 epoxy resin. The SQUID reading out the MMC signal is placed next to the MMC chip.

2.2 Source and Absorber Preparation Techniques

The source preparation is fundamental for the precise measurement of beta spectra with MMCs. It must ensure that the entire energy of every beta particle is deposited and thermalized in the absorber.

The best source preparation approach—besides implanting the radionuclide directly into the absorber material—is electrodeposition forming a metallic layer. For many elements, however, an oxide/hydroxide layer will form during electrodeposition. This can still be a high-quality source consisting in a very thin layer. Within this project, ^{151}Sm and ^{99}Tc sources were fabricated by electrodeposition.

Where electrodeposition is not possible, as is the case of ^{14}C or ^{36}Cl, drop-deposited sources were produced. The common manual drop deposition often leads to the formation of large (~ micrometers) salt crystals. Previous studies using MMCs have revealed that salt crystals can cause considerable spectrum distortion due to incomplete thermalization [7]. The formation of large salt crystals can be avoided if the required activity is deposited in a 2D array of very small individual droplets. Commercial micro-dispensing systems can deposit single droplet volumes of less than 50 pl in combination with a placement accuracy of better than 20 µm. With such a system, ^{36}Cl, ^{99}Tc and ^{14}C were deposited onto gold foils preformed into absorber arrays by milling techniques, with lateral dimensions of individual absorber elements of about 0.7 mm and 1.6 mm. Figure 2a shows an absorber array after the radioactive solution was dried. Volumes of 100 nl (left half) and 50 nl (right half) of a ^{99}Tc solution were deposited in the middle of each marked absorber. The

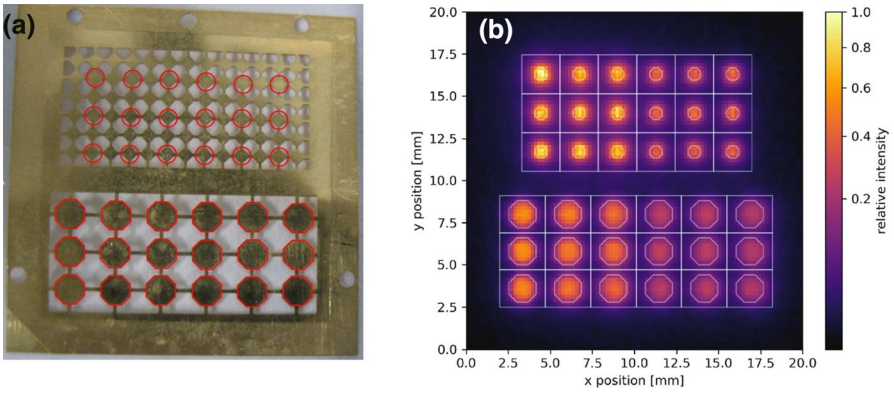

Fig. 2 **a** Photograph of an array of pre-fabricated gold absorber foils with ^{99}Tc sources deposited by a microdrop dispenser system in the middle of the marked absorbers. **b** Autoradiography image of the same array. Two different activity levels, 5 Bq/2.5 Bq, have been deposited on each marked absorber in the left/right half of the array. (Color figure online)

autoradiography image in Fig. 2b confirms the position and the different activities of the deposited material.

Fine dispersion of the source material in the absorber metal will also improve the source quality compared to a conventional drop-deposited source. This can be achieved by alternate folding and laminating of the foil with the source deposit, breaking the source crystals into tens of nanometer small particles that are embedded in the metal foil [8]. This technique was applied to the electrodeposited ^{151}Sm source, because it had a black aspect and was considered not to be ideally thin.

Monte Carlo simulations—see Sect. 4—indicate that spectrum distortion of higher energy beta spectra by escape of bremsstrahlung from the absorber can be reduced by embedding the beta emitter into bilayer absorbers with an inner layer of lower atomic number and an outer layer of high atomic number (e.g., copper, $Z=29$, and gold, $Z=79$). Preparing this kind of absorbers requires several steps of diffusion welding under vacuum or inert gas to avoid oxidation of the copper.

3 Beta Spectrum Measurements

Three beta spectra have been measured using MMCs within the MetroBeta project; the more challenging ^{36}Cl measurements are under way.

3.1 ^{14}C

The spectrum of ^{14}C ($Q=156.476$ keV) has been measured using a source prepared as described in Ref. [5]. The absorber (Au, 1 mm$^2\times(2\times25$ µm)) was placed on an MMC chip best matching its heat capacity (34 pJ/K at 10 mK). The experimental conditions during the measurement were far from optimal. During the cooling phase, the glue layer fixing the MMC chip to its holder broke; the chip was then only suspended by the gold and aluminum bonding wires used for electric and thermal contacts. Hence, the MMC could vibrate, resulting in an energy resolution near 200 eV (FWHM), approximately five times worse than expected from the absorber heat capacity. Nevertheless, the detector performance was much better than in the measurement published in [5]: The energy resolution was improved by a factor of five, while the energy threshold was reduced from ~ 5 to ~ 700 eV. Figure 3 shows the experimental spectrum containing 2.7 million events together with a theoretical spectrum calculated with the code BetaShape [9, 10].

3.2 ^{151}Sm

A ^{151}Sm source was electrodeposited on a 10-µm-thick silver foil, forming a Sm oxide/hydroxide layer. After the mechanical processing described in Sect. 2.2, this source foil (0.8 mm × 0.8 mm × 7 µm) was sandwiched between two silver foils (0.9 mm × 0.9 mm × 15 µm each, total absorber heat capacity: 14.5 pJ/K at 10 mK). The performance of the MMC during this measurement was as expected: The

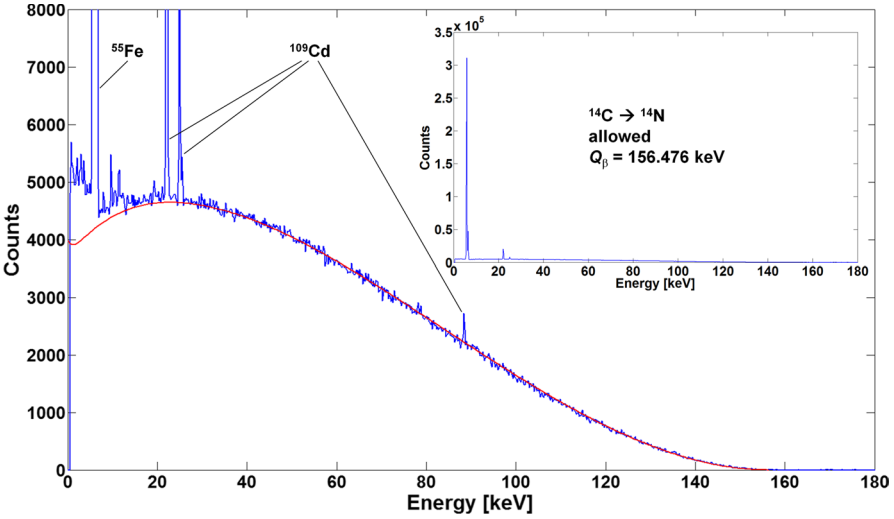

Fig. 3 Beta spectrum of ^{14}C measured with an MMC (*blue*). The discrete lines are X-ray and gamma ray lines from an external ^{55}Fe + ^{109}Cd energy calibration source. The inset shows the unclipped spectrum with the energy calibration lines in full height. A theoretical spectrum calculated with the code BetaShape is shown in red. The deviation of the experimental spectrum at low energies may be attributed to the degraded detector performance. (Color figure online)

energy resolution ranges from 45 eV (FWHM) at 6 keV to 70 eV at 25 keV, and the energy threshold is 250 eV.

^{151}Sm has a main β^- decay branch ($Q_\beta = 76.4$ keV) to the ground state and a second β^- decay branch to the 21.54 keV excited level of ^{151}Eu. The recommended values for the probabilities of the two decay paths are 99.07 (4) % and 0.93 (4) % [11]. The de-excitation of the 21.54 keV excited state leads to the emission of gamma rays (3.4% of the decays), respectively, to the emission of conversion electrons and subsequently X-rays and/or Auger electrons. The detector absorber stops all conversion electrons, more than 99% of all X-rays and more than 95% of the 21.54 keV gamma photons. The result is that for practically all beta decays to the excited level, the sum of the beta energy and the gamma energy is absorbed. Thus, the measured spectrum for the decays to the excited level is shifted by the energy of the gamma transition and starts at 21.54 keV, leading to a step in the recorded spectrum. Since the maximum energy for this beta branch equals the Q value minus the gamma transition energy, the end point of both measured spectra is the same, 76.4 keV. As it is not possible to distinguish events from the two decay branches, both spectra are superimposed in one experimental spectrum.

The measured spectrum (10.2 million events) is shown in Fig. 4 together with theoretical spectra calculated with the code BetaShape for both decay paths. The area between the two theoretical spectra, corresponding to the probability of the decay to the excited state of ^{151}Eu, amounts to 2.6% of the total, in clear contradiction with the recommended value. Concerning the spectrum shape, the discrepancy between experiment and theory at low energies is most likely due to an incomplete

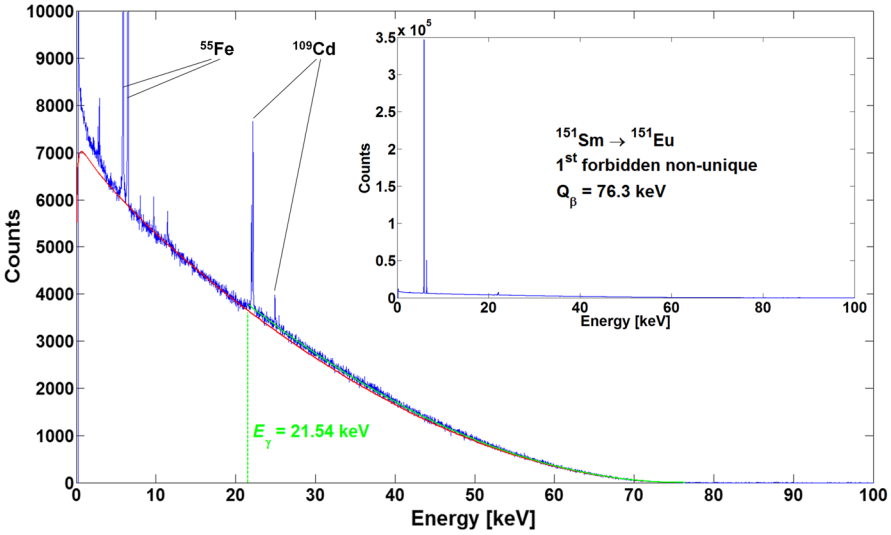

Fig. 4 Beta spectrum of ^{151}Sm measured with an MMC (*blue*) together with theoretical spectra calculated for the beta decay to the ground state (*red*) and to the 21.54 keV excited level of ^{151}Eu (*green*). The inset shows the unclipped spectrum with the energy calibration lines in full height. (Color figure online)

control of the atomic effects in the theoretical calculation of this first forbidden, non-unique transition.

3.3 ^{99}Tc

The beta spectrum of ^{99}Tc ($Q = 293.8$ keV) was measured both at PTB and at LNHB.

At LNHB, a ^{99}Tc source was electrodeposited on gold, forming metallic technetium. This source foil was sandwiched between two gold foils (0.9 mm × 0.9 mm × 74 µm each, $C_{abs} = 175$ pJ/K at 10 mK). Data were acquired during 13.7 days, and the spectrum contains 5.65 million events. The energy resolution is practically energy independent, about 100 eV (FWHM) up to 384 keV, the energy of the highest energy gamma ray line of a ^{133}Ba source used for energy calibration and check of the linearity. Comparing the measured and the tabulated line energies between 31 keV and 384 keV shows no larger deviations than 70 eV, less than the energy resolution, and no obvious trend.

At PTB, ^{99}Tc sources were prepared with a microdrop dispenser directly on a 90-µm-thick gold absorber array (Fig. 2a). An identical array was diffusion welded onto the array with the sources. One of the larger absorbers ($C_{abs} = 545$ pJ/K at 20 mK) was glued onto a matching MMC. The spectrum after 42 h of data acquisition consists of 0.5 million events with an energy threshold of about 5 keV and an energy resolution of 600 eV at the 122 keV gamma line of a ^{57}Co energy calibration source. The larger absorber heat capacity, vibrations from the pulse tube cooler and

bath temperature instability explain the degraded energy resolution and threshold compared to the measurement performed at LNHB.

Figure 5 shows a superposition of both experimental spectra; the spectrum shape is practically the same. The theoretical spectrum that is also shown in Fig. 5 has been calculated with the current version of the code BetaShape, supposing an allowed transition, and multiplied with an experimental shape factor [12]. It is not surprising that this shape factor, derived from a measurement with an energy threshold of 55 keV, cannot correctly reproduce the spectrum at lower energies. It is noteworthy that the spectrum measured at LNHB has an energy threshold of 650 eV.

4 Toward the Measurement of ^{36}Cl

For beta spectra with maximum energies higher than a few 100 keV, potential distortion of the measured spectra by the escape of bremsstrahlung must be considered. In first order, the radiative energy loss of the beta particles scales linearly with energy. Hence, the higher the beta Q value, the stronger the spectrum distortion will be. In principle, this distortion can be corrected for via Monte Carlo simulation; however, the bremsstrahlung cross sections needed for the simulations suffer from high uncertainties.

Since the bremsstrahlung production scales with the square of the atomic number Z, a low Z absorber material may be a good candidate in view of minimizing this source of spectrum distortion. On the other hand, a low Z absorber needs to

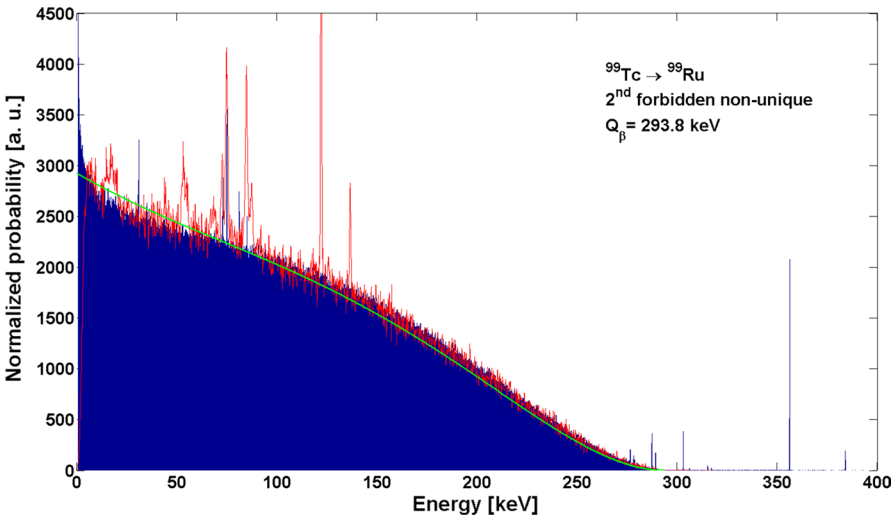

Fig. 5 Beta spectrum of ^{99}Tc resulting from two fully independent measurements and data analyses. *Blue histogram*: measured at LNHB (Laboratoire National Henri Becquerel, France) and *red line*: measured at PTB (Physikalisch-Technische Bundesanstalt, Germany). All lines in the blue spectrum are from a ^{133}Ba energy calibration source (including some escape peaks); all lines in the red spectrum are from a ^{57}Co energy calibration source. A theoretical spectrum calculated with the code BetaShape and using a shape factor from Ref. [12] is also shown (*green*). (Color figure online)

be significantly larger in order to stop the beta particles, thus implying larger heat capacity, and is moreover less efficient for the reabsorption of at least a fraction of the bremsstrahlung photons. A composite absorber composed of an inner layer of a low Z material, reducing the bremsstrahlung production near the beta emitter where the beta particles have still high energy, and an outer layer of a high Z material, reducing the overall absorber heat capacity compared with a monolithic low Z absorber and more efficiently reabsorbing photons, may be an interesting option combining the advantages of both low and high Z.

To test this hypothesis, a series of Monte Carlo simulations have been performed using the PENELOPE code [13] for the case of ^{36}Cl ($Q = 709.53$ keV). Five types of absorber comprising elements with three different atomic numbers were simulated: monolithic gold ($Z = 79$), silver ($Z = 47$) and copper ($Z = 29$), and composite absorbers with an inner copper or silver layer and an outer gold layer. For each absorber type, in a first step the minimal necessary absorber thickness was determined by means of lower statistics simulations only at the maximum energy of ^{36}Cl. In a second step, the resulting absorber was simulated with a central 100-nm-thick NaCl layer acting as a source layer spiked with the active ^{36}Cl. Electrons with initial energies following a theoretical spectrum based on the experimental ^{36}Cl spectrum from Ref. [1] were generated in the source layer; the result of the simulation is the distribution of the energies deposited in the absorber, i.e., the expected spectrum that would be measured with each absorber.

Figure 6 presents the five simulated spectra together with the initial theoretical spectrum. It can be clearly seen that the spectrum distortion is highest for the monolithic gold absorber (~ 1.5% in the energy range 100–200 keV) and becomes smaller with lower Z. One can also observe that the spectrum distortion in the composite silver (resp. copper)–gold absorber is smaller than in the monolithic silver (resp. copper) absorber. The smallest distortion is obtained with the copper–gold bilayer absorber.

A first attempt with a ^{36}Cl source prepared on a copper foil and embedded subsequently between two copper–gold bilayers was made; unfortunately, the detector did not perform as expected and no exploitable spectrum could be measured. New measurements with both gold and copper–gold bilayer absorbers will be performed shortly and compared with the Monte Carlo simulations.

5 Conclusions and Perspectives

Within the European Metrology Research Project MetroBeta, developments of both MMCs and source/absorber preparation techniques for beta spectrometry have been conducted. Several spectra with end-point energies ranging from ~ 76 to 294 keV were measured, and the measurements of ^{36}Cl ($Q_\beta = 709$ keV) are ongoing. It was demonstrated that MMC measurements also have the potential to yield valuable information about other decay scheme parameters such as the probability of the beta decay from ^{151}Sm to the excited level of ^{151}Eu. Thus, MMC spectrometry of radionuclides with more complex decay schemes is an interesting extended research field

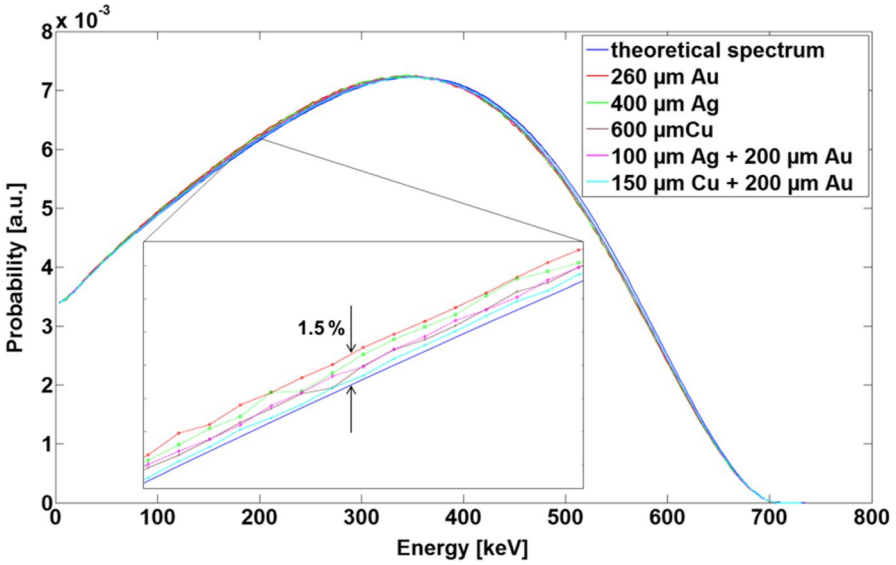

Fig. 6 Simulation of the spectrum distortion due to the escape of bremsstrahlung in the case of the beta spectrum of ^{36}Cl ($Q = 709.53$ keV). The initial spectrum based on Ref. [1] is shown in dark blue. Five types of absorbers were simulated: Au (red), Ag (green), Cu (brown), Ag–Au bilayer (magenta) and Cu–Au bilayer (cyan). The layer thicknesses are indicated in the figure. For better visibility, the inset shows a zoom into the energy range 150–200 keV. (Color figure online)

[14]. Studies indicate that ^{129}I, ^{204}Tl and ^{210}Pb are promising candidates for such measurements which should yield valuable nuclear decay data.

Acknowledgements This work was performed as part of the EMPIR Project 15SIB10 MetroBeta. The project has received funding from the EMPIR program co-financed by the Participating States and from the European Union's Horizon 2020 research and innovation program.

References

1. H. Rotzinger, M. Linck, A. Burck, M. Rodrigues, M. Loidl, E. Leblanc, L. Gastaldo, A. Fleischmann, C. Enss, J. Low Temp. Phys. **151**, 1087 (2008)
2. M. Loidl, M. Rodrigues, B. Censier, S. Kowalski, X. Mougeot, P. Cassette, T. Branger, D. Lacour, Appl. Radiat. Isot. **68**, 1454 (2010)
3. M. Loidl, C. Le-Bret, M. Rodrigues, X. Mougeot, J. Low Temp. Phys. **176**, 1040 (2014)
4. http://metrobeta-empir.eu/
5. M. Loidl, J. Beyer, L. Bockhorn, C. Enss, D. Györi, S. Kempf, K. Kossert, R. Mariam, O. Nähle, M. Paulsen, M. Rodrigues, M. Schmidt, J. Low Temp. Phys. **193**, 1251 (2018)
6. S. Kempf, A. Fleischmann, L. Gastaldo, C. Enss, J. Low Temp. Phys. **193**, 365 (2018)
7. C. Le-Bret, M. Loidl, M. Rodrigues, X. Mougeot, J. Bouchard, J. Low Temp. Phys. **167**, 985 (2012)
8. A.S. Hoover et al., Anal. Chem. **87**, 3996–4000 (2015)
9. X. Mougeot, C. Bisch, Phys. Rev. A **90**, 012501 (2014)
10. X. Mougeot, Phys. Rev. C **92**, 059902 (2015)
11. M.-M. Bé et al., Table of Radionuclides, Monographie BIPM-5, vol. 8 (2016), ISBN-13 978-92-822-2264-5

12. M. Reich, H.M. Schüpferling, Z. Phys. **271**, 107–113 (1974)
13. F. Salvat et al., PENELOPE A code system for Monte Carlo simulation of Electron and Photon transport, Rapport NEA/NSC/DOC (2001) 19
14. P. C.-O. Ranitzsch, D. Arnold, J. Beyer, L. Bockhorn, J. J. Bonaparte, C. Enss, K. Kossert, S. Kempf, M. Loidl, R. Mariam, O. J. Nähle, M. Paulsen, M. Rodrigues, M. Wegner, J. Low Temp. Phys. This Special Issue (2019). https://doi.org/10.1007/s10909-019-02278-4